
AFRL-AFOSR-VA-TR-2018-0388

# Canonical Shear Flow Interactions with Unsteady Airfoils

**Manoochehr Koochesfahani**
**MICHIGAN STATE UNIVERSITY**

**09/13/2018**
**Final Report**

**DISTRIBUTION A: Distribution approved for public release.**

Air Force Research Laboratory
AF Office Of Scientific Research (AFOSR)/ RTA1
Arlington, Virginia 22203
Air Force Materiel Command

DISTRIBUTION A: Distribution approved for public release

# REPORT DOCUMENTATION PAGE

*Form Approved*
*OMB No. 0704-0188*

**The public reporting burden for this collection of information is estimated to average 1 hour per response, including the time for reviewing instructions, searching existing data sources, gathering and maintaining the data needed, and completing and reviewing the collection of information. Send comments regarding this burden estimate or any other aspect of this collection of information, including suggestions for reducing the burden, to Department of Defense, Executive Services, Directorate (0704-0188). Respondents should be aware that notwithstanding any other provision of law, no person shall be subject to any penalty for failing to comply with a collection of information if it does not display a currently valid OMB control number.**
**PLEASE DO NOT RETURN YOUR FORM TO THE ABOVE ORGANIZATION.**

| 1. REPORT DATE *(DD-MM-YYYY)* | 2. REPORT TYPE | 3. DATES COVERED *(From - To)* |
|---|---|---|
| 12-10-2018 | Final Performance | 15 Jun 2015 to 14 Jun 2018 |

**4. TITLE AND SUBTITLE**
Canonical Shear Flow Interactions with Unsteady Airfoils

**5a. CONTRACT NUMBER**

**5b. GRANT NUMBER**
FA9550-15-1-0224

**5c. PROGRAM ELEMENT NUMBER**
61102F

**6. AUTHOR(S)**
Manoochehr Koochesfahani

**5d. PROJECT NUMBER**

**5e. TASK NUMBER**

**5f. WORK UNIT NUMBER**

**7. PERFORMING ORGANIZATION NAME(S) AND ADDRESS(ES)**
MICHIGAN STATE UNIVERSITY
426 AUDITORIUM RD, RM 2
EAST LANSING, MI 48824-2600 US

**8. PERFORMING ORGANIZATION REPORT NUMBER**

**9. SPONSORING/MONITORING AGENCY NAME(S) AND ADDRESS(ES)**
AF Office of Scientific Research
875 N. Randolph St. Room 3112
Arlington, VA 22203

**10. SPONSOR/MONITOR'S ACRONYM(S)**
AFRL/AFOSR RTA1

**11. SPONSOR/MONITOR'S REPORT NUMBER(S)**
AFRL-AFOSR-VA-TR-2018-0388

**12. DISTRIBUTION/AVAILABILITY STATEMENT**
A DISTRIBUTION UNLIMITED: PB Public Release

**13. SUPPLEMENTARY NOTES**

**14. ABSTRACT**

A coordinated experimental and computational investigation is carried out to determine how the basic flow physics of steady and unsteady airfoils are altered when the upstream approach flow is changed from the traditional uniform conditions to that of non-uniform flow. Our particular objectives are to establish the alterations that occur for both the load on the airfoil and also the flow field structure. This work considers the NACA 0012 airfoil in pure pitch with low to moderate angle of attack amplitudes about zero mean angle of attack, and chord Reynolds number of order 10,000. It is found that a steady symmetric airfoil has negative lift at zero angle of attack when placed in steady shear flow with positive shear, opposite of the prediction of inviscid theory. A hypothesis is formulated to explain the observed sign of the lift force on the basis of the asymmetry in boundary layer development on the upper and lower surfaces of the airfoil, which creates an effective airfoil shape with negative camber. However, it is found that the same steady airfoil placed in the unsteady flow field of a two-stream shear layer generates positive lift at zero angle of attack. Also, the character of the (CL - alpha) curve changes fundamentally and the multi-slope features of the curve in the case of uniform flow completely disappear in favor of a much longer linear region characteristic of much higher Reynolds number airfoils. The main influence of shear approach flow on unsteady aerodynamic load is on the mean lift, leaving the mean thrust and force fluctuations mostly unaffected.

**15. SUBJECT TERMS**
shear flow, unsteady, pitching airfoil, plunging airfoil, molecular tagging velocimetry, gust

Standard Form 298 (Rev. 8/98)
Prescribed by ANSI Std. Z39.18

DISTRIBUTION A: Distribution approved for public release

| 16. SECURITY CLASSIFICATION OF: | | | 17. LIMITATION OF ABSTRACT | 18. NUMBER OF PAGES | 19a. NAME OF RESPONSIBLE PERSON |
|---|---|---|---|---|---|
| a. REPORT | b. ABSTRACT | c. THIS PAGE | | | ABATE, GREGG |
| Unclassified | Unclassified | Unclassified | UU | | 19b. TELEPHONE NUMBER *(Include area code)* 703-588-1779 |

Standard Form 298 (Rev. 8/98)
Prescribed by ANSI Std. Z39.18

DISTRIBUTION A: Distribution approved for public release

# Canonical Shear Flow Interactions with Unsteady Airfoils

Manoochehr Koochesfahani and Ahmed Naguib

Department of Mechanical Engineering
Michigan State University
East Lansing, Michigan

**Air Force Office of Scientific Research**
**Grant No. FA9550-15-1-0224**

**Final Technical Report**

14-September-2018



DISTRIBUTION A: Distribution approved for public release

## 1. Background

This investigation is motivated by the need to understand the changes that can occur in steady and unsteady airfoil aerodynamics caused by disturbances in the upstream approach flow. Current understanding of both steady and unsteady aerodynamics is based on a uniform freestream velocity approaching the airfoil. The classical unsteady theory of oscillating airfoils, based on linearized inviscid analysis [1,2], and extensions that incorporate nonlinear processes of wake vorticity roll-up using numerical techniques [3-5] rely on a uniform far-field velocity boundary condition. Practically all fundamental studies of unsteady aerodynamics, both experimental [e.g. see 6-11] and computational [e.g. see 12-19] use a uniform approach velocity. Unsteady freestream boundary condition has been used for theories and studies related to transient response of an airfoil to sudden change in approach speed, periodic changes in freestream speed, or gust response [see summary in Ref. 20]. The approach velocity, though unsteady, is still spatially uniform in all these studies.

There are many situations where the condition of a uniform approach velocity is a very poor approximation. These situations include wings near the ground, wind shear, ambient wind conditions that are altered by large scale disturbances (e.g. mountains), and aircraft operating in close proximity, among others. The work of Tsien in 1943 [21] was among the earliest to investigate the influence of non-uniform upstream conditions by considering a linear velocity profile (uniform shear) approaching a steady 2-D symmetric Joukowsky airfoil. His inviscid analysis showed that the effect of uniform shear is a shift in the zero-lift angle of attack (AoA) such that a symmetric airfoil at zero AoA in an approach flow with positive shear generates positive lift. This work was subsequently extended to more general velocity profiles [22-24], but all of these studies are limited to inviscid steady flows. Systematic studies of the influence of upstream shear on airfoil aerodynamics in real viscous flows are hard to find. One exception is the wind tunnel experiments of Payne & Nelson [25] on a steady airfoil in uniform shear at chord Reynolds numbers on order of $10^5$. It is difficult to conclusively determine the influence of shear on the angle of zero lift based on the reported data. The complexities caused by a non-uniform approach flow on the flow structure and load on unsteady airfoils have not been investigated in a methodical way. As a result, there are practically no fundamental guidelines on how the known basic flow features of an unsteady airfoil, even for 2-D airfoils, get modified in the presence of spatially non-uniform approach flow. To this end, our proposal considers canonical configurations of upstream shear flow boundary condition and targets to isolate the ensuing fundamental flow interactions and their influence on steady and unsteady aerodynamics.

## 2. Objectives

The focus of this research effort is to determine how the basic flow physics of steady and unsteady airfoils are altered when the upstream approach flow is changed from the traditional uniform conditions to that of non-uniform flow. Our particular objectives are to establish the alterations that occur for both the load on the airfoil and also the flow field structure. In this study we consider unsteady airfoils in pure pitch and low to moderate angle of attack amplitudes.

Consideration of the general case of non-uniform approach flow is not a well-defined and tractable problem. Instead, we focus on exploring the fundamental aspects and interactions based on simpler canonical configurations of upstream flow non-uniformity in order to provide



DISTRIBUTION A: Distribution approved for public release

guidance for more complex situations. Two classes of canonical flows are considered as our upstream boundary condition: 1) approach flow with linear velocity profile (i.e. uniform shear rate), which also provides a connection to Tsien's inviscid theory, and 2) the plane two-stream shear layer. This research program is conducted as a joint experimental and computational effort, where experiments are carried out alongside complementary computations of the same problem with initial and boundary conditions that are matched as closely as possible. This complementary approach of closely-coordinated experiment and computation has proven invaluable in our previous AFOSR-supported research on unsteady aerodynamics. The computational aspects build on our existing and fruitful collaboration with Miguel Visbal and the high-fidelity simulation group at AFRL. Details of experimental implementation and computational approach are given in the next section.

## 3. Methods

### *3.A. Shear Profile Characteristics*

The inviscid theory of Tsien is based on a shear profile that extends to infinity, a boundary condition that is difficult to reproduce in the current computations since at high enough shear rates the velocities, and corresponding Mach numbers, become extremely large away from the airfoil (positive in the upper domain and negative in the lower). It is also incredibly challenging to create the equivalent boundary condition for experiments, especially the reverse flow profile below the airfoil. Therefore, our work utilizes a 3-segment profile as the boundary condition, where the uniform shear zone (and its linear velocity profile) occurs over a finite region of thickness $\delta$ and the velocities outside this region are uniform. The details are shown schematically in Figure 1. This composite profile is now characterized by the non-dimensional shear rate $K = (c/U_o)\,(dU_\infty/dy)$ introduced by Tsien [21] and the additional parameter $\delta/c$. In the case of plane two-stream shear layer, the mean velocity profile in the self-similar region is well approximated by the hyperbolic tangent profile (see Figure 2). In this case, we characterize the profile in terms of its vorticity thickness $\delta_\omega = \Delta u/(dU_\infty/dy)_{max}$, where $\Delta u = U_1 - U_2$ is the velocity difference across the shear layer, and its maximum non-dimensional shear rate $K_{max} = (c/U_o)\,(dU_\infty/dy)_{max}$. Note that for uniform shear $\delta_\omega \equiv \delta$ and $K_{max} \equiv K$.

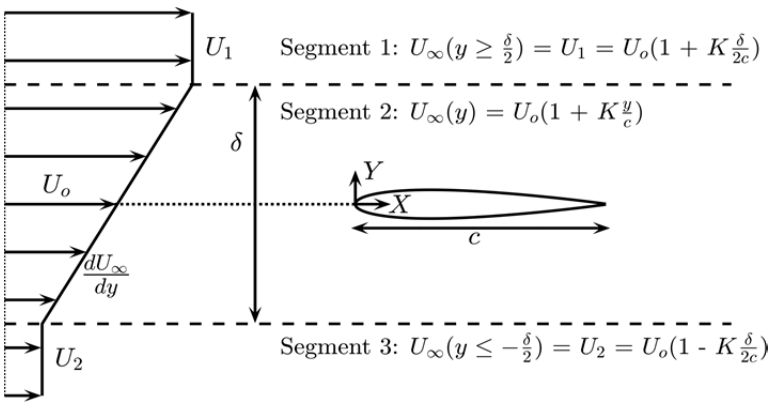


Figure 1. Schematic of the 3-segment linear velocity profile used for the upstream boundary condition.

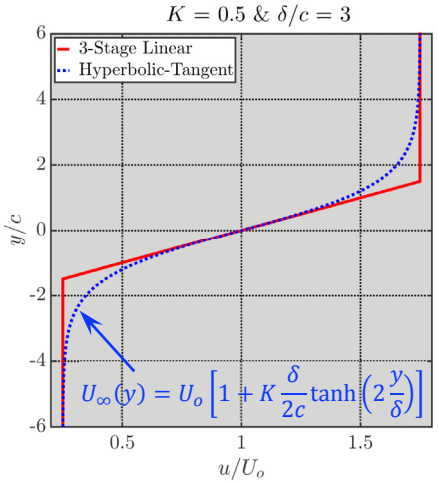


Figure 2. Hyperbolic tangent profile in comparison to the 3-segment linear velocity profile.



DISTRIBUTION A: Distribution approved for public release

### *3.B. Methods of Shear Generation in the Approach Flow*

Among the various methods for creation of non-uniform velocity profile in a flow facility, e.g. curved screens [26], array of parallel rods [27], and variable length honeycomb [28], we opted for the latter because of its better suitability to our water tunnel facility and also lower turbulence level generation. We have developed a design methodology, based on an extension of the original work of Kotansky [28] for generation of linear profile (uniform shear), that allows us to create velocity profiles of arbitrary shape inside a wind/water tunnel. In this methodology, the variable-length honeycomb profile shape is computed to create the appropriate pressure drop variation that results in the desired velocity profile downstream of the honeycomb [29].

We demonstrate the shaped honeycomb approach for shear generation with a device that was designed to generate a hyperbolic tangent velocity profile with centerline speed $U_o$= 10 cm/s in our ¼-scale (15 cm × 15 cm test section) water tunnel. The actual shape of the honeycomb predicted by the methodology, shown in Figure 3, was cut from a rectangular block using specialized band saw blade. Figure 4 depicts the development of the time-averaged velocity profile from the exit of the honeycomb device to a distance $x/d \approx 62$, where $d$ is the honeycomb cell diameter. As expected, the flow at the exit of the honeycomb is dominated by the individual jets coming out of each honeycomb cell, but quickly smooths out, and after a distance of 62 cell diameters the presence of individual jets is non-existent, with the measured velocity profile matching the design profile quite closely.

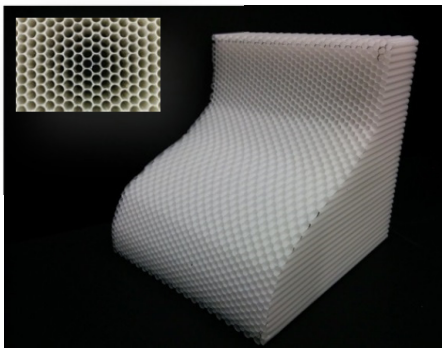

Figure 3. Shaped honeycomb shear generation device designed to generate a hyperbolic tangent mean velocity profile.

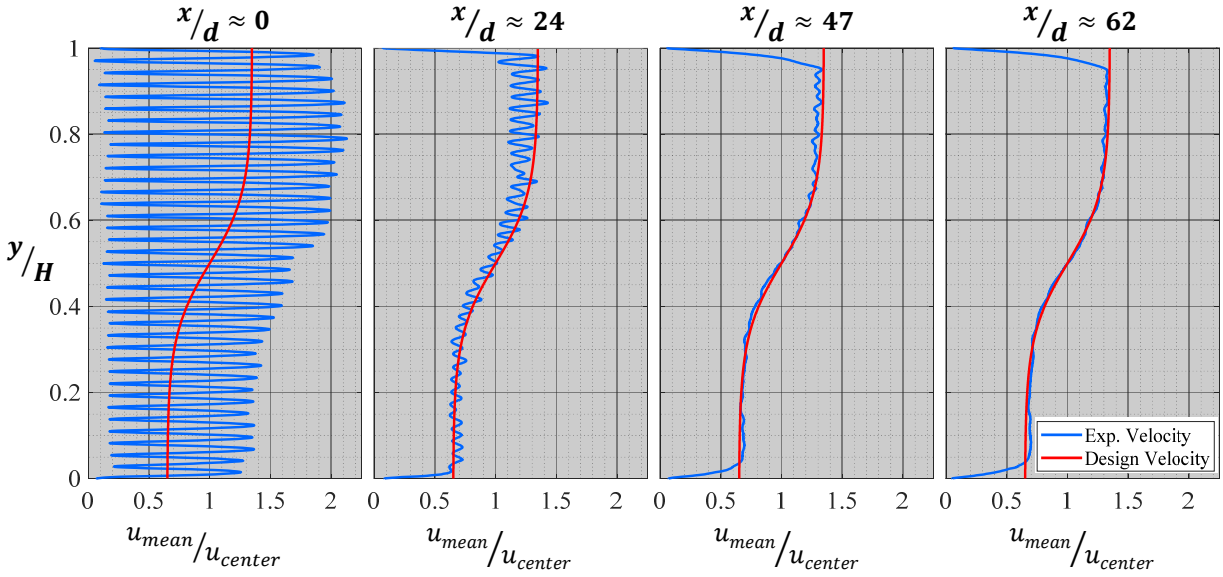


Figure 4. Measured time-averaged velocity profile evolution downstream of the shaped honeycomb in comparison with the design velocity profile. $H$ is the test section size (15 cm), and $d$ is the honeycomb cell diameter (≈ 3.2 mm).



DISTRIBUTION A: Distribution approved for public release

Quantitatively, it is found that after a distance of roughly 60 honeycomb cell diameters ($x/d \approx 60$), spatial deviations from a smooth hyperbolic tangent profile fall within 1% of the centerline velocity. An interesting characteristic of the shear profile thus generated is its spatially uniform velocity fluctuation ($u_{rms}$) profile. As illustrated in Figure 5, the $u_{rms}$ profile of the hyperbolic tangent velocity profile at $x/d \approx 62$ is nearly uniform across the entire profile, similar to the baseline undisturbed freestream characteristic of the water tunnel, but at a fluctuation level that is slightly below that of the baseline turbulence level naturally present in the water tunnel. As a result, we have been referring to shear flows created by the shaped honeycomb device as "steady" shear flows, in contrast to the non-uniform $u_{rms}$ profile in plane two-stream shear layers and its high turbulence level in the center of the shear layer (see sections that follow). In addition, in all the shear flows we have created with this method thus far, whether a linear shear profile or hyperbolic tangent, over the downstream regions investigated the shear layer stays straight in orientation and the growth of its width is negligibly small. The ability to create such steady shear flows is fortunate since it allows us to isolate the influence of mean shear in the approach flow on airfoil aerodynamics.

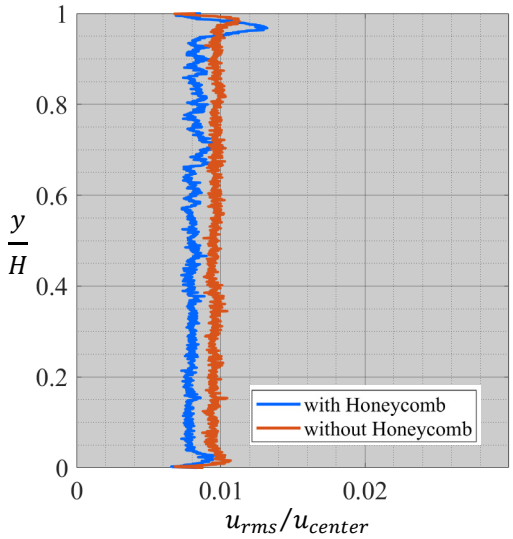

Figure 5. Measured velocity fluctuation profile at downstream location $x/d \approx 62$.

The second canonical shear flow boundary condition in our studies is the plane two-stream shear layer. It is created here by the two-stream splitter-plate approach, where two streams of different speeds are initially separated by a thin splitter plate and they subsequently form the plane two-stream shear layer downstream of the splitter plate tip. The initial two streams of different speeds are created using two blocks of honeycombs with different length, such that their different pressure drops lead to the two desired freestream stream speeds. The shear layer created mimics the behavior of classical canonical two-stream shear layers [30-32]. The behavior of such shear layers is very well-studied and they are known to contain vortical structures.

We now show the characteristics of the plane two-stream shear layer with velocity ratio $U_1/U_2 = 2$ that was created in our full-scale (61 cm × 61 cm test section) water tunnel. The initial wake component of the velocity profile, created by the boundary layers on the two sides of the splitter plate, almost completely disappears after $x \approx 40$ cm downstream of the splitter plate. The growth of the shear layer width beyond this location, shown in Figure 6 in terms of the downstream evolution of its vorticity thickness, adheres to the linear

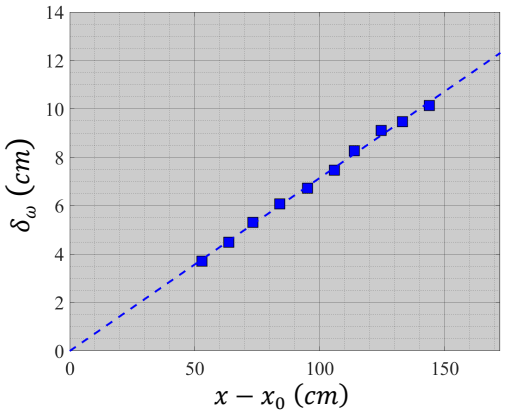

Figure 6. Downstream growth of the two-stream shear layer thickness. $x_o$ is the shear-layer's virtual origin location.



DISTRIBUTION A: Distribution approved for public release

growth behavior of canonical two-stream shear layers. The measured growth rate of $d\delta_\omega/dx = 0.071$ is consistent with the reported literature [32]. The normalized mean and rms velocity profiles, which are illustrated in Figure 7 at several locations after the wake component has disappeared, also demonstrate the self-similar characteristics of the canonical shear layer. Note in Figure 7 the non-uniform nature of the velocity fluctuation profile and its high fluctuation level compared to the uniform and low fluctuation counterpart in the case of the "steady" shear flow (see Figure 5). The peak velocity rms in the plane two-stream shear layer in Figure 7 is about a factor 20 higher than that in the "steady" shear flow of Figure 5.

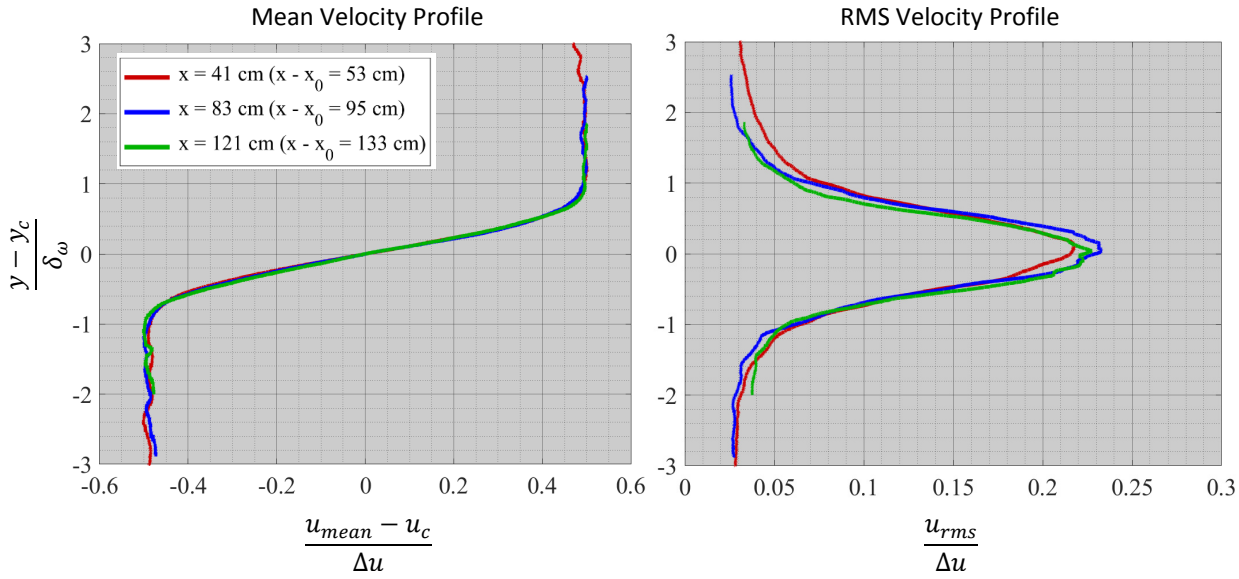


Figure 7. Self-similar behavior of the normalized mean and rms velocity profiles in the two-stream shear layer. $\Delta u = U_1 - U_2$ is the velocity difference across the shear layer, $u_c = (U_1 + U_2)/2$ is the speed at the shear layer center location $y_c$ , and $x_o$ is the shear-layer's virtual origin location.

### *3.C. Experimental Setup*

The experiments are conducted in a closed-return 61 cm × 61 cm free-surface water tunnel at the Turbulent Mixing and Unsteady Aerodynamics Laboratory (TMUAL) at Michigan State University. The tunnel is fitted with a three-degree-of-freedom (3 DOF) servo motion system that is capable of producing pitch, heave and surge motion. Only the pitch motion is utilized in the present work. A NACA 0012 airfoil with chord length $c$ = 12 cm and high aspect ratio $AR$ = 5.14 is attached to the pitch axis via a force balance, as depicted in Figure 8. The shaft connecting the airfoil to the balance, passes through a "skimmer plate" (not shown in figure), which skims the water free surface and spans the full test-section width to avoid disturbing the free surface during airfoil oscillation, and to provide a well-defined boundary condition on the top side of the airfoil. Less than a 0.5 mm clearance gap is left between the top end of the airfoil and the skimmer plate, on one hand, and the bottom end of the airfoil and the test section floor, on the other. The pitch motor is fitted with a high-resolution encoder that captures the airfoil pitch angle with a resolution of 0.003 degrees. To generate the desired upstream shear flow boundary condition, the shear generation device based on the two methods described in Section



DISTRIBUTION A: Distribution approved for public release

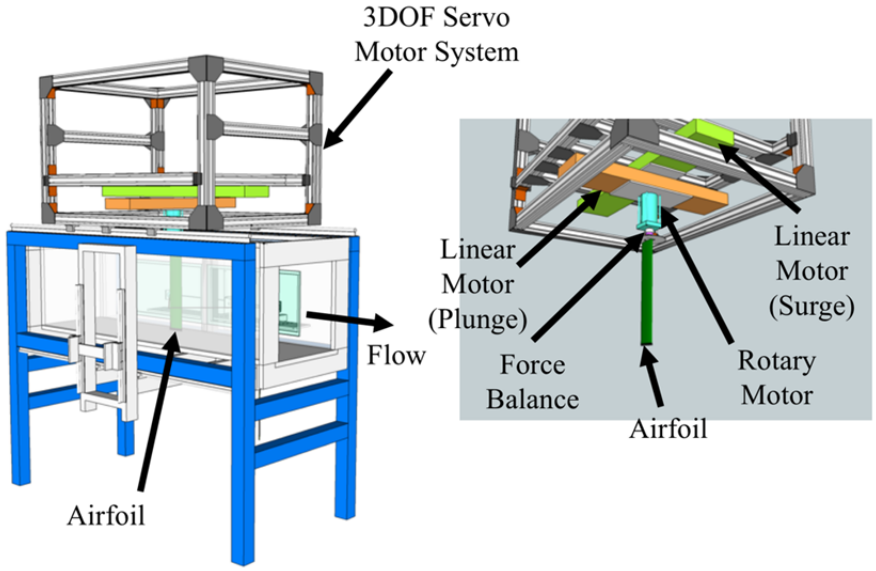


Figure 8. Water tunnel test section, showing the vertical airfoil mounted to the 3 DOF servo motion system on top of the test section (left), along with the details of the 3 DOF system and airfoil mounting (right).

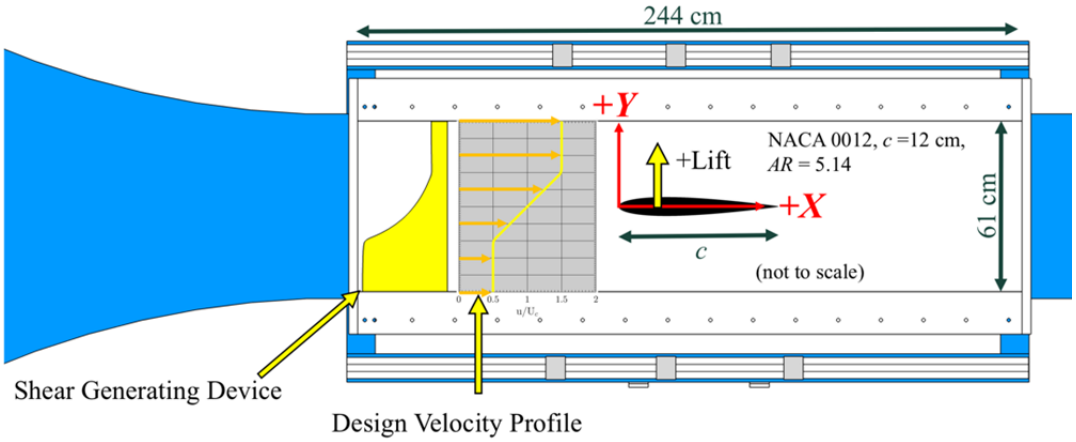


Figure 9. Top view of the test section showing placement of the shear generation device, and the resulting shear flow approaching the NACA 0012 airfoil.

3B is placed in the path of the uniform flow at the test section entrance (see Figure 9). The characteristics of the generated shear profile are carefully documented in terms of the downstream evolution of the mean and rms velocity profiles using molecular tagging velocimetry (MTV).

Load measurements are carried out using an ATI Mini40 six-component force balance/load cell. To account for the inertia forces produced during oscillatory pitching due to the mass of the airfoil, support shaft, and other components mounted on the pitch axis, force measurements are conducted with the airfoil placed in still air while executing the same pitch oscillations as used in the water tunnel tests. Results from these measurements are found to be negligible (primarily due



DISTRIBUTION A: Distribution approved for public release

to the axially aligned center of mass of all sub-components) and are, therefore, not generally utilized. Also, "flow-off" measurements of forces are conducted in the water tunnel immediately preceding and following the "flow-on" measurements. The duration of each experiment is kept to less than 15 minutes such that load cell drift is also negligibly small (less than the resolution reported below). The resolution, based on sensor specifications, of lift/drag force measurements is 0.005 N for the Mini 40, corresponding to lift/drag coefficient resolution of 0.014. The uncertainty of the mean force coefficient measurements for the static airfoil tests is estimated to be 0.005 based on the standard error of the mean and accounting for drift over the duration of each measurement. The capability of our setup for accurate load measurements was verified by comparing our measurements of the load on a circular cylinder at different Reynolds numbers against published data in the literature [33].

### *3.D. Computational Method*

All computations are performed using the extensively validated high-order *FDL3DI* Navier-Stokes solver [34,35], which was developed at the Computational Sciences Branch, AFRL Wright-Patterson Air Force Base. The code solves the full, compressible, unsteady, three-dimensional Navier-Stokes equations. A finite-difference approach is used to discretize the governing equations, and all spatial derivatives are obtained with high-order compact-differencing schemes [36]. A sixth-order scheme is used at interior points, whereas at boundary points, higher-order one-sided formulas are invoked which retain the tridiagonal form of the scheme. In order to eliminate spurious components, a high-order low-pass spatial filter is incorporated [34,35]. Finally, time-marching is accomplished by incorporating an iterative, implicit approximately-factored procedure [37-40]. We have previously used this solver very effectively in studies of 2-D unsteady airfoil aerodynamics in the incompressible limit in the case of uniform approach flow. Details can be found in [41] in terms of grid resolution, Mach number, time step, convergence, and validation studies.

The boundary conditions are enforced as follows. No-slip, adiabatic condition is applied to the surface in conjunction with zero-normal pressure gradient at the wall. For these studies with non-uniform approach flow, prescribed streamwise velocity profile $U_\infty(y)$, uniform static pressure, and uniform total temperature are specified along the upstream far-field boundary. At the three additional far-field boundaries, first-order accurate extrapolation condition is applied to the primitive variables, except for pressure, which is uniform. Spatial periodicity is enforced in the azimuthal direction of the O-mesh around the airfoil using a five-point overlap. For steady airfoil studies, the solution is initialized with the specified velocity profile, uniform static pressure, and uniform total temperature everywhere in the domain. For unsteady airfoils, the computation is initialized using the converged solution for the steady airfoil at zero angle of attack. Further details of the computational procedure and results for the case of shear flow approaching steady and unsteady airfoils are given in [42-44].



DISTRIBUTION A: Distribution approved for public release

## 4. Results

The material in this section represents only selected cases from our studies to highlight the main results from this research effort to date. Data are discussed primarily for the case of airfoil chord Reynolds number of $Re_c = U_o\, c/\upsilon = 1.2 \times 10^4$, based on the centerline velocity $U_o$ at the ¼-$c$ pitch axis. In the case of unsteady airfoil, we consider pure pitch sinusoidal oscillation about the ¼-$c$ axis with zero mean angle of attack (AoA) and amplitude $\alpha_o = 2°$. Results are first described for the case of "steady" shear flow as the upstream boundary condition approaching either the steady or unsteady airfoil. Subsequently, we give our early results for the case of plane two-stream shear layer as the boundary condition upstream of the steady/unsteady airfoil. This component of the investigation is still ongoing.

### *4.A. "Steady" Shear Flow as Upstream Approach Flow*

This part of our study focuses on the 3-segment linear velocity profile as the upstream approach flow (see Figure 1). It considers primarily the case of large enough $\delta/c$ (typically in the range 1.5 – 2) so that the finite size of the shear zone does not influence the results and Tsien's theory [21] provides the inviscid solution.

#### *4.A.1 Steady Airfoil at Zero Angle of Attack*

The computed average lift coefficient $C_L$ at zero AoA versus shear rate $K$ is shown in Figure 10 for the viscous solution of NACA 0012 airfoil at $Re_c = 1.2 \times 10^4$ in comparison to its inviscid solution using the panel method [43]. The accuracy of the panel code is demonstrated to be excellent when tested against Tsien's exact solution for 12% thick Joukowsky airfoil (J 12); see Figure 10. Note that the inviscid $C_L$ for NACA 0012 increases linearly with $K$ just as the 12% thick Joukowsky airfoil, but with a slope that is higher by 12.8%, a consequence of the shape difference between these airfoils.

The most important result from Figure 10 is that the behavior of the viscous solution is fundamentally different from its inviscid counterpart. In the former, the sign of lift is *negative* (i.e. downward force), which is *exactly opposite of the inviscid prediction*. Its magnitude, however, increases with shear rate $K$ in a nearly linear fashion. We note in this figure that increasing the size of the shear zone by a factor of two to $\delta/c = 3.0$ has a minimal impact on the lift force, indicating that $\delta/c = 1.5$ is a sufficiently large value. The influence of upstream shear on drag coefficient is found to be weak; results (not shown here) indicate that $C_D$ decreases monotonically with increasing $K$, with $C_D$ at $K = 1.0$ dropping by only 2% compared to its value for uniform flow ($K = 0.0$).

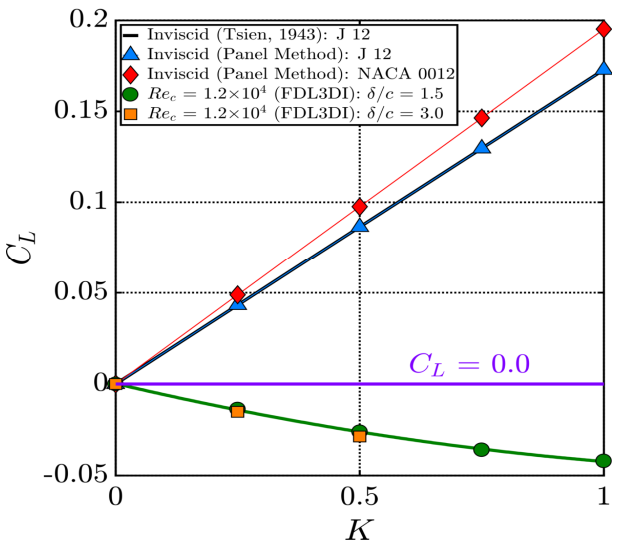


Figure 10. Average lift coefficient $C_L$ at zero AoA vs shear rate $K$ for NACA 0012 airfoil at $Re_c = 1.2 \times 10^4$ in comparison to the inviscid solution [43]. The inviscid NACA 0012 and 12% thick Joukowsky airfoil (J12) solutions are both included.



DISTRIBUTION A: Distribution approved for public release

Our hypothesis for generation of negative lift at zero AoA for a symmetric airfoil placed in a flow with positive shear is connected to the asymmetry of boundary layer development on the upper and lower surfaces of the airfoil. In positive shear, the upper boundary layer grows in a region with higher freestream velocity compared to that on the lower surface, resulting in a thicker boundary layer on the lower surface than the upper surface. The resulting difference between the corresponding displacement thicknesses effectively creates an airfoil with negative camber (camber towards the low-speed side), leading to negative lift. A first-order analysis of the resulting effect using laminar boundary layer relations for attached flow, in conjunction with classical inviscid airfoil analysis, leads to an estimate of the *additional* lift caused by the effective camber to be negative and given as $C_L \sim -\frac{1}{\sqrt{Re_c}} K \left(\frac{t}{c}\right)$ [43]. We note that the effective camber, and therefore also the resulting lift magnitude, in this first-order model, is linear in both shear rate $K$ and airfoil thickness ratio $t/c$ and decreases as $1/\sqrt{Re_c}$. In this description, the lift of a symmetric airfoil at zero AoA in viscous flow with positive shear will always be lower than its inviscid counterpart (i.e. Tsien's theory) by the expression given above. The results in Figure 10 for $Re_c = 1.2 \times 10^4$ imply that the lift reduction due to negative camber at this Reynolds number is large enough to change the positive lift prediction of Tsien's theory to negative lift.

The simple model described allows us to give an estimate for how high the chord Reynolds number should be before the inviscid theory of Tsien becomes applicable. According to the model, the chord Reynolds number needs to be as high as $Re_c = 2.0 \times 10^6$ in order to get to 90% of inviscid prediction [43]. This estimate is consistent with the trend in our computations at higher chords Reynolds numbers of up to $10^6$ [45] even though this model and its prediction are constrained by its assumptions of laminar and attached flow, which cease to be uniformly valid over the curved surfaces of the airfoil as the Reynolds number varies.

The results reveal several other interesting flow field asymmetries that develop due to imposed shear (see Reference 43). For example, the location of leading edge stagnation point moves increasingly farther back along the airfoil's upper surface with increased shear rate, a behavior consistent with a negatively-cambered airfoil. Furthermore, the symmetry in the location of boundary layer separation point on the airfoil's upper and lower surfaces in uniform flow is broken under imposed shear. The wake vortical structures exhibit more asymmetry with increasing shear rate, as depicted in Figure 11. Interestingly, however, natural shedding Strouhal

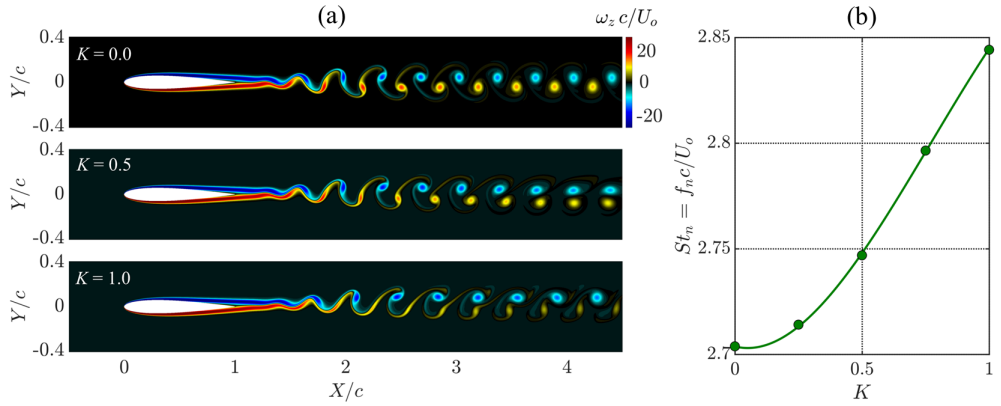


Figure 11. Influence of upstream shear on (a) the instantaneous spanwise vorticity field ($\omega_z c/U_o$) and (b) the natural shedding Strouhal number $St_n$. Solid line represents a curve fit to data.



DISTRIBUTION A: Distribution approved for public release

number changes very little over the range of shear rates investigated.

The discovery of the negative lift on a symmetric airfoil at zero AoA when it is placed in an approach flow with positive shear has been confirmed by our experiments [33,44]. These experiments used the shaped honeycomb approach to create a 3-segment linear velocity profile with $K = 0.5$, $\delta/c = 2$ as the upstream approach flow in the water tunnel. A lower shear rate could be also obtained from the same device by simply adding a fine mesh screen after the exit of the honeycomb device. Comparison of computed and measured results is shown in Figure 12. The computations include both the data from Figure 10, as reference, and also new data based on using the experimentally measured upstream shear profile boundary conditions created by the shear generation device. The excellent agreement between the experiment and computation is noteworthy.

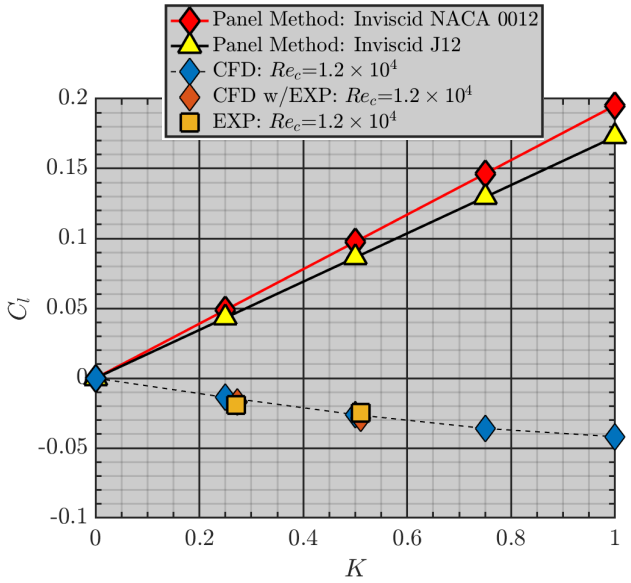


Figure 12. Comparison of experimentally measured and computed lift coefficient $C_L$ at zero AoA vs shear rate $K$ for NACA 0012 airfoil at $Re_c = 1.2 \times 10^4$. The inviscid NACA 0012 and 12% thick Joukowsky airfoil (J12) solutions are both included.

*4.A.2. Unsteady Airfoil*

Results are described in this section for the NACA 0012 airfoil pitching sinusoidally about the ¼-$c$ axis with zero mean angle of attack (AoA) and amplitude $\alpha_o = 2°$. The oscillation reduced frequency, $k = 2\pi fc/U_o$, where $f$ is the oscillation frequency, varies from 0 to approximately 12. The upstream approach shear flow is the 3-segment linear velocity profile with $\delta/c = 1.5$, with non-dimensional shear rate $K$ varying between zero (i.e. uniform flow) and one. Selected highlights of the results are given here, while more extensive details are found in Reference [44].

The influence of upstream shear on the airfoil wake structure is visualized in Figure 13 using instantaneous spanwise vorticity $\omega_z$ fields for the uniform ($K = 0.0$) and the shear ($K = 1.0$) flow.



DISTRIBUTION A: Distribution approved for public release

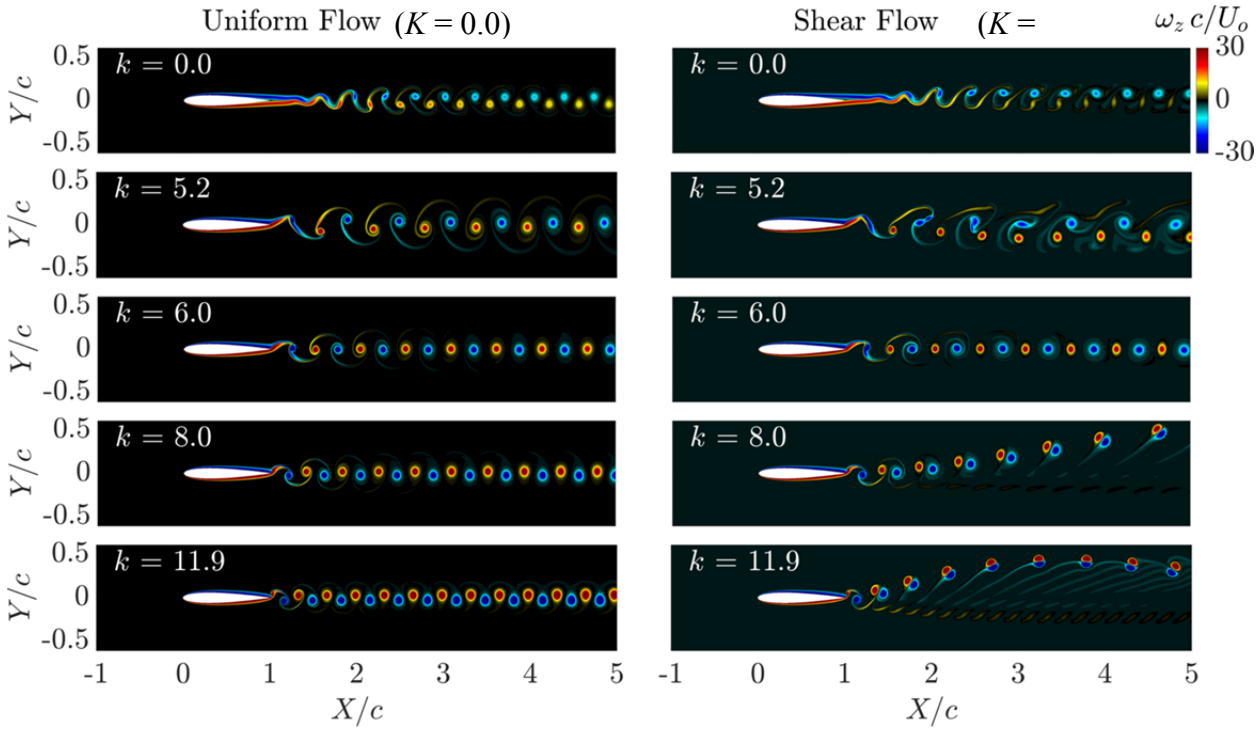


Figure 13. Instantaneous spanwise vorticity fields for $K = 0.0$ (left) and 1.0 (right), with increasing reduced frequency from top to bottom. The airfoil is at zero angle of attack and is pitching up.

As seen previously in Figure 11, the steady airfoil ($k = 0$) in uniform flow produces a von Kármán vortex street, while the wake structure for the shear case has asymmetry, with the stronger vorticity having the same sign as the vorticity produced by the approach shear flow. At reduced frequency $k = 5.2$, the uniform flow case also produces a von Kármán vortex street, with more well-defined vortices and connecting braids than in the steady airfoil case. The shear case at this value of $k$ shows a much more distorted structure but with the wake configuration remaining in the traditional von Kármán street formation at farther downstream locations. When the reduced frequency increases to $k = 6.0$, the wake vortices are nearly aligned with the wake centerline (i.e. neutral wake) for *both* the uniform and shear flow cases. It is interesting that the formation of the neutral wake is not influenced by the presence of upstream shear. At $k = 8.0$ and 11.9, the vortices in the uniform flow case take on the reverse von Kármán vortex street pattern. With upstream shear, the vortices are also in the reverse von Kármán vortex street configuration (in the sense that the positive vortex is located above the negative one), but the pattern deflects upward towards the high-speed-side. The angle of vortex pattern upward deflection visually increases as $k$ increases. Wake structure deflection due to shear in the approach flow was also observed in Reference [46], but at a much lower Reynolds number of $3.0\times10^3$.

The primary influence of upstream shear flow on the load on the oscillating airfoil is summarized in Figure 14 in terms of mean lift $C_L$ and its peak-to-peak fluctuation $C_{L,pp}$ and thrust $C_T$ and its peak-to-peak fluctuation $C_{T,pp}$ . Note that a negative value of thrust implies drag force. In the case of uniform upstream flow, the average lift coefficient is zero across the entire range of $k$, as expected. The average thrust coefficient begins at negative values (i.e., drag force), decreases in magnitude as $k$ increases, switches sign to become positive, and then increases in magnitude.



DISTRIBUTION A: Distribution approved for public release

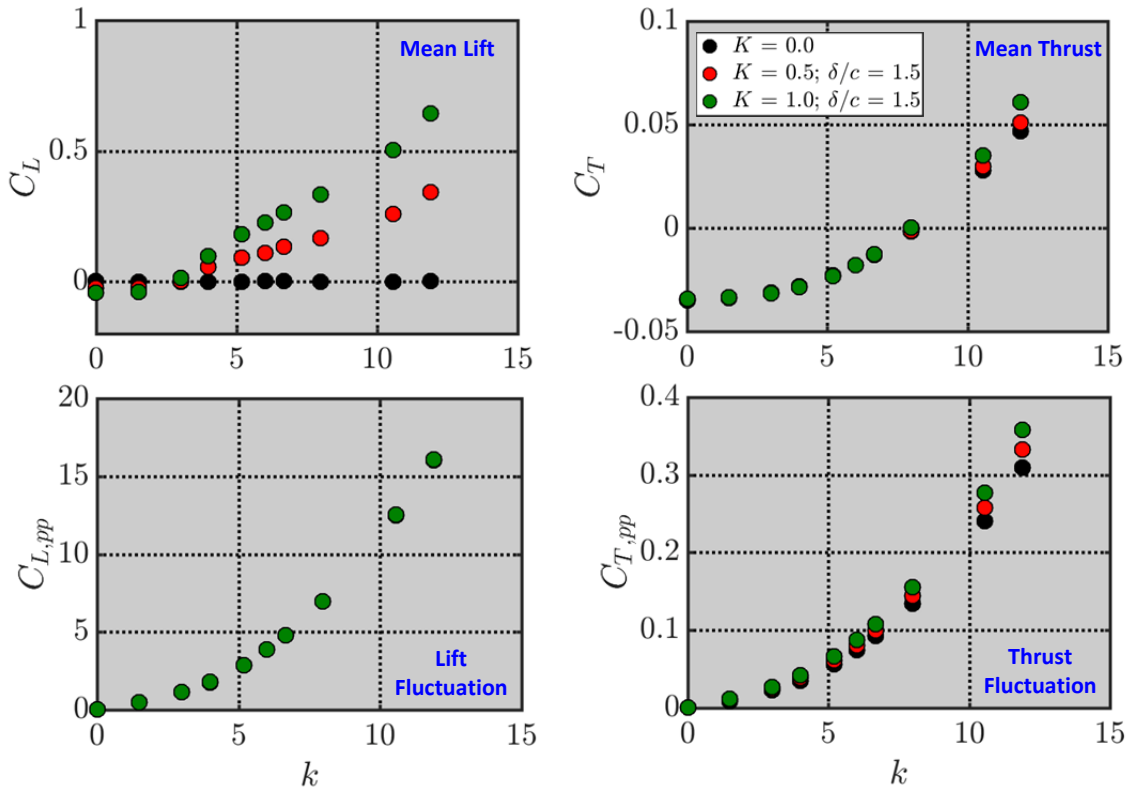


Figure 14. Influence of upstream shear $K$ on the variation of mean and fluctuating lift and thrust forces versus oscillation reduced frequency $k$. Upstream shear profile is 3-segmented linear profile with $\delta/c = 1.5$.

This trend reflects the well-known switch of the mean streamwise force from drag to thrust with increasing reduced frequency. As expected, the lift and thrust fluctuation amplitudes increase as $k$ increases.

The most important observation from Figure 14 is that the asymmetry caused by upstream shear creates positive mean lift above a certain reduced frequency ($k \approx 3$ in this case), whose magnitude increases with both shear rate and oscillation reduced frequency. On the other hand, lift fluctuation is not affected and stays identical to that in uniform flow. The mean and fluctuating thrust force are also weakly affected by upstream shear for the cases studied here. It is noteworthy that the generation of non-zero lift does not coincide with the development of a deflected wake shown in Figure 13. Moreover, for cases where the wake does deflect, the sign of the lift is contrary to that expected from the wake deflection direction. These observations are similar with the behavior seen previously in the case of deflected wakes in uniform flow caused by a plunging airfoil, where the connection between deflection direction and sign of lift is counter-intuitive; specifically, that the wake deflection is in the same direction as the lift force [47].

The results of Figure 14 have been corroborated by complementary experiments with the 3-segmented linear profile as upstream boundary condition. Data shown in Reference [44] indicate excellent quantitative agreement between the experimental measurements of lift and drag and the



DISTRIBUTION A: Distribution approved for public release

computed results, with the exception of some discrepancy in the thrust fluctuation level at the highest reduced frequencies considered.

### *4.B. Plane Two-Stream Shear Layer as Upstream Approach Flow*

The results we present in this section are based on experiments that were recently conducted. Computational aspects of this work are still being developed as it is a lot more challenging to create the upstream flow field boundary condition that captures the various flow details of a two-stream shear layer.

The characteristics of the plane two-stream shear layer we have created were previously described in Section 3B. Several distinctions exist between this upstream flow boundary condition and the case of "steady" shear flow for which we showed results in Section 4A. Apart from the non-uniform velocity fluctuation profile and its high fluctuation level in a two-stream shear layer compared to the uniform and low fluctuation counterpart in the case of the "steady" shear flow, the two-stream shear layer mean velocity profile grows linearly downstream, whereas the "steady" shear flow in our studies has negligible downstream growth. As a result, the downstream placement of the airfoil in the two-stream shear layer allows us to vary the value of $\delta_\omega/c$ and $K_{max}$. The particular locations of the airfoil for which we show results in this report are in the self-similar region of the shear layer and they are indicated in Figure 15. We also point out that the range of $\delta_\omega/c$ values in this case (0.5 – 0.9) is noticeably smaller than the values in the range 1.5 – 2.0 that was discussed for the work with "uniform" shear flow boundary condition.

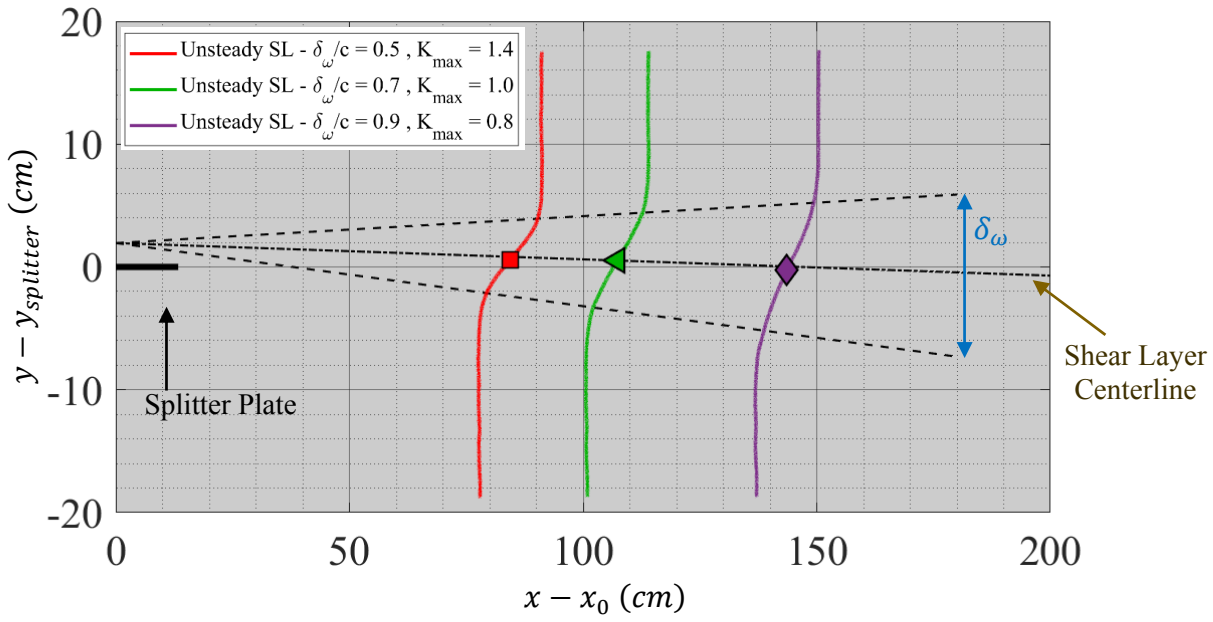


Figure 15. Locations of the airfoil in the plane two-stream shear layer and corresponding values of $\delta_\omega/c$ and $K_{max}$.



DISTRIBUTION A: Distribution approved for public release

*4.B.1 Steady Airfoil*

Before presenting the influence of the two-stream shear layer on the aerodynamics of the steady airfoil, we first discuss the results for the case of "steady" shear layer to provide reference data against which to compare. Figure 16 presents experimental data of ($C_L$ - $\alpha$) curve over an extended AoA range (±20°) to illustrate the influence of "steady" shear flow boundary condition in comparison with uniform approach flow. The shear flow profile is the 3-segmented linear profile described previously with $\delta_\omega/c \equiv \delta/c = 2.0$ and $K_{max} \equiv K = 0.5$ .

The ($C_L$ - $\alpha$) curve in Figure 16 for the case of uniform flow exhibits a multi-slope character that is typical for the airfoil Reynolds number in this study. When the upstream approach flow changes to the "steady" shear flow, the general multi-slope features of ($C_L$ - $\alpha$) curve remain unchanged. However, noticeable asymmetry develops as the AoA magnitude increases, with the largest changes occurring in the negative AoA region. The enlarged view of the small AoA region shows the presence of negative lift at zero AoA, a feature that was extensively discussed in Section 4.A.1.

The influence of the two-stream shear layer approach flow on the ($C_L$ - $\alpha$) curve is fundamentally different in several ways compared to those just described for our "steady" shear flow. As shown in Figure 17, the character of the ($C_L$ - $\alpha$) curve is now completely changed. The multi-slope features in the case of uniform flow completely disappear and the ($C_L$ - $\alpha$) curve now resembles the behavior of much higher Reynolds number airfoils, in that it now has a much longer linear

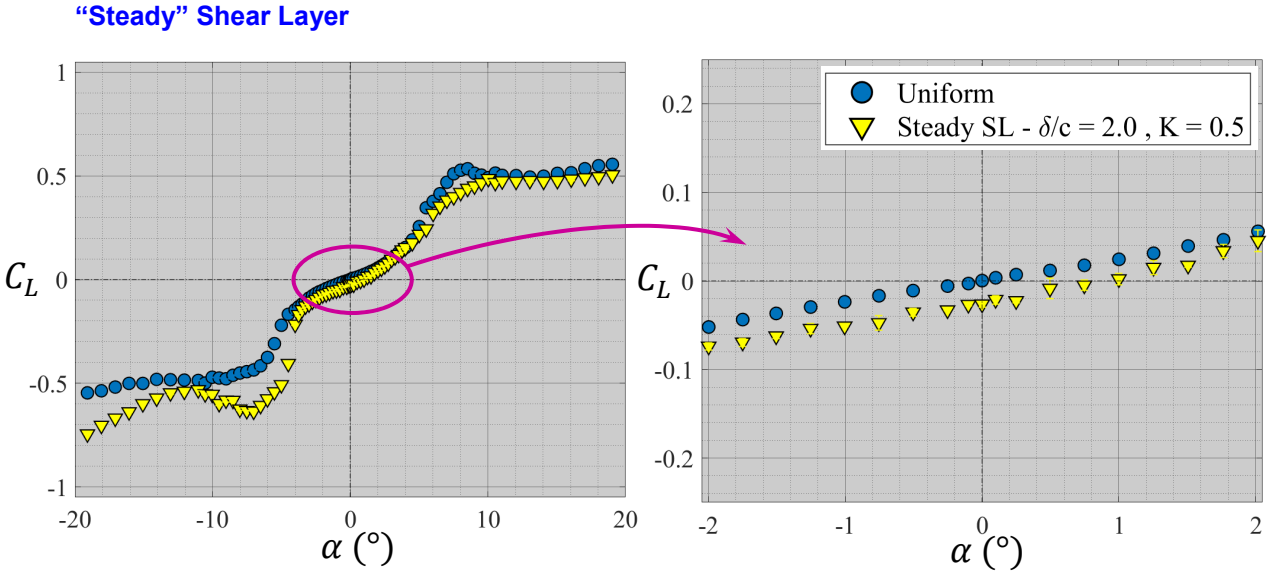


Figure 16. Influence of "steady" shear flow approach stream on the variation of lift coefficient with AoA in comparison with uniform approach flow for NACA 0012 airfoil at $Re_c$ = 1.2 × $10^4$. Upstream shear profile is the 3-segmented linear profile. Enlarged view of small AoA region is shown on the right.



DISTRIBUTION A: Distribution approved for public release

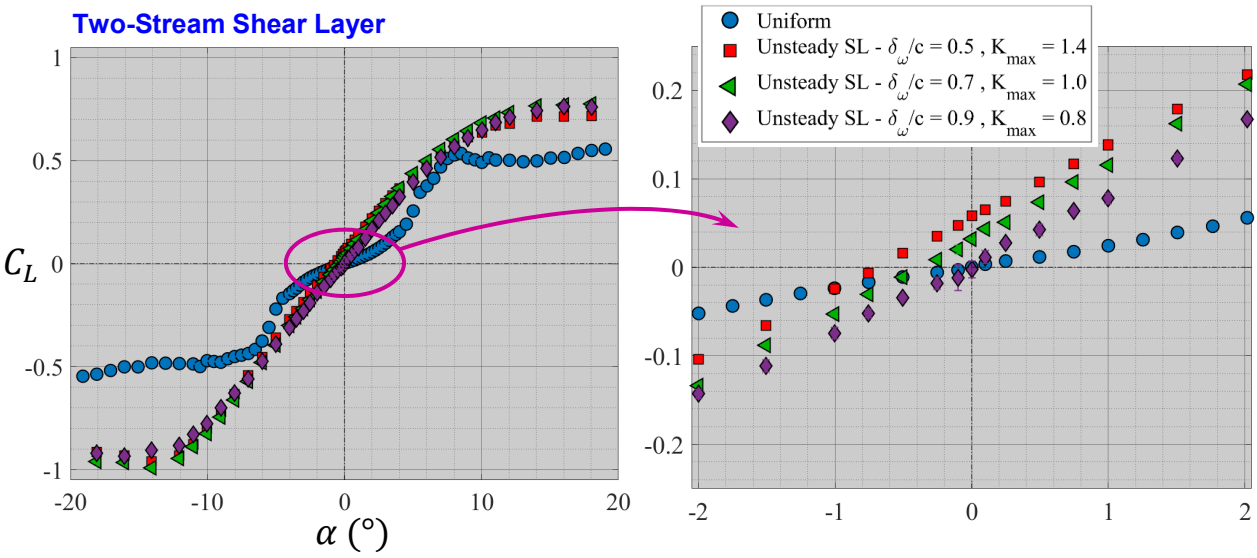


Figure 17. Influence of two-stream shear layer approach stream on the variation of lift coefficient with AoA in comparison with uniform approach flow for NACA 0012 airfoil at $Re_c = 1.2 \times 10^4$. Enlarged view of small AoA region is shown on the right.

region around zero AoA. There is also a much larger increase in the lift coefficient at high angles of attack, with the largest change occurring in the negative AoA region. Finally, upon examining the region near zero AoA, we note that the value of lift at zero AoA is NO LONGER negative, the feature that was prominent in the case of "steady" shear flow approaching the airfoil. With the two-stream shear layer approach flow, $C_L$ at zero AoA is now positive and its magnitude decreases with increasing $\delta_\omega/c$ and decreasing $K_{max}$ .

The underlying physical mechanisms behind these intriguing results are not clear at this time. There are several, possibly interconnected, elements that can be playing a role. They include the high level of fluctuation in the approach flow and its non-uniformity, the possible role of the shear layer large-scale vortical structure dynamics, the small shear zone thickness relative to airfoil chord and high shear rates. Work is continuing to try to isolate the influence of these effects.

*4.B.2. Unsteady Airfoil*

Results are described for the pitching NACA 0012 airfoil at two locations within the two-stream shear layer, the most upstream and downstream locations indicated in Figure 15. As before, we are considering sinusoidal pitching about the ¼-$c$ axis with zero mean angle of attack (AoA) and amplitude $\alpha_o = 2°$.

Results are summarized in Figure 18 in terms of the measured mean and fluctuating lift and thrust coefficients versus oscillation reduced frequency. For comparison, the results for the cases of uniform freestream and the "steady" shear flow approach stream are also included. Several interesting features are readily apparent. The asymmetry caused by the two-stream shear layer



DISTRIBUTION A: Distribution approved for public release

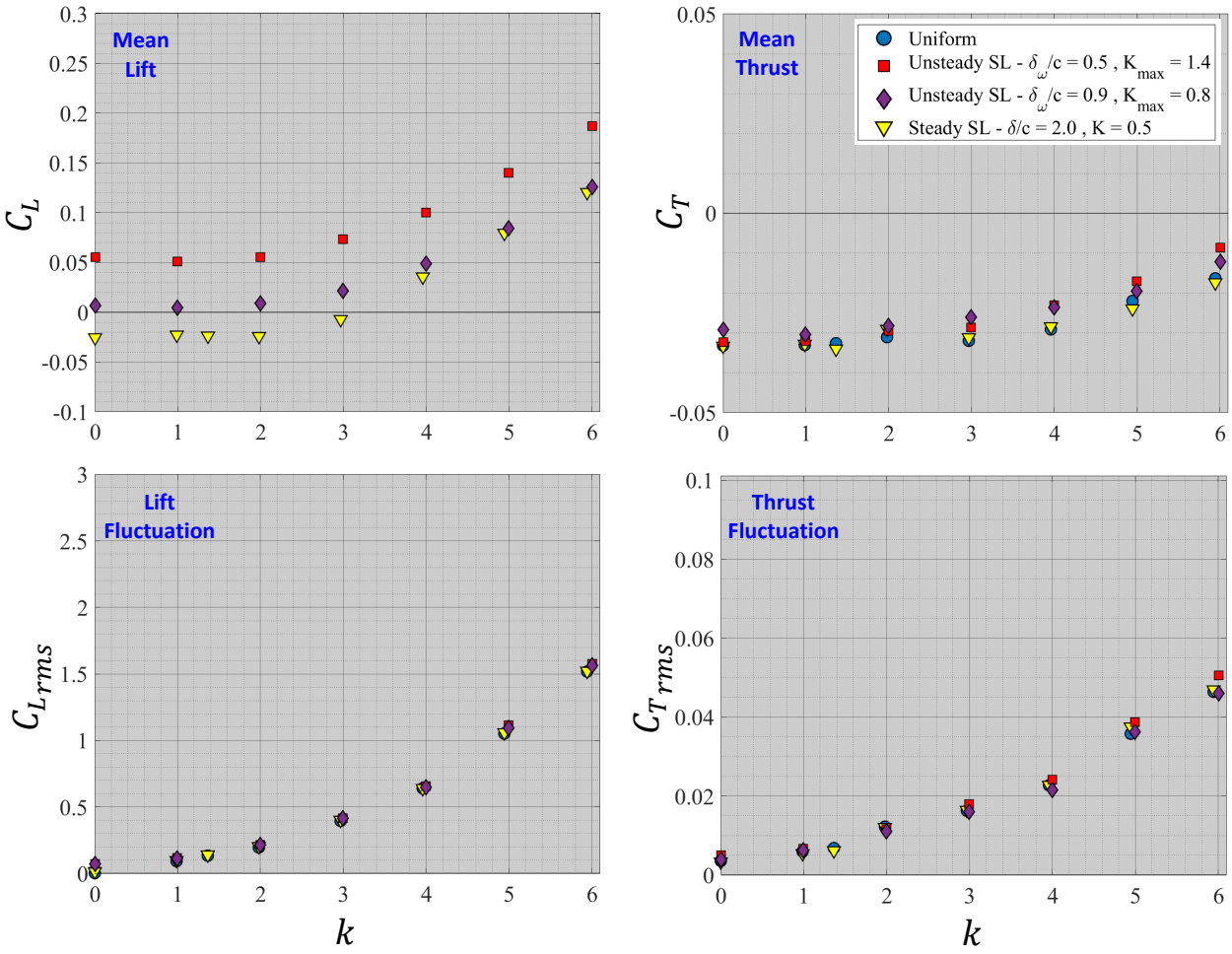


Figure 18. Influence of the two-stream shear layer approach flow on the variation of mean and fluctuating lift and thrust forces versus oscillation reduced frequency $k$. Results are included for two downstream locations in the shear layer, along with data for uniform freestream and "steady" shear flow approach stream.

causes the mean lift, which is initially positive for steady airfoil (i.e. $k = 0$), to start to increase further above a certain reduced frequency ($k \approx 3$ in this case), with the magnitude of additional lift increasing with the oscillation reduced frequency. The latter result is the same finding we described for the case of "steady" shear flow boundary condition, even though the mean lift starts with a negative value for steady airfoil in that case. Interestingly, the lift fluctuation variation with reduced frequency is not affected by the form of upstream boundary condition; two-stream shear layer, "steady" shear flow, and uniform freestream all lead to nearly identical lift fluctuation level at a given reduced frequency. Similarly, the mean thrust and its fluctuation level are weakly affected by the upstream boundary conditions we have studied here.

The investigation of the two-stream shear layer approach flow is still continuing in order to clarify the fundamental flow physics that underlie the interesting results we have just described.



DISTRIBUTION A: Distribution approved for public release

## 5. Publications

Publications that have resulted from this project are listed below. The list includes publications that have appeared already, as well as those under preparation.

*5.A. Publications*

1. Hammer, P., Visbal, M., Naguib, A., Koochesfahani, M. [2018] "Lift on a steady 2-D symmetric airfoil in viscous shear flow," *J. Fluid Mech*., **837**, R2 (11 pp) (doi:10.1017/jfm.2017.895)
2. Hammer, P. R., Olson, D. A., Visbal, M. R., Naguib, A. M., and Koochesfahani, M. M. [2018] "An Investigation of the Aerodynamics of a Harmonically Pitching Airfoil in Uniform-Shear Approach Flow," *AIAA* Paper No. AIAA 2018-0575.

*5.B. Conference Presentations*

1. Olson, D., Naguib, A., and Koochesfahani, M. [2016] "Experiments on a Steady Low Reynolds Number Airfoil in a Shear Flow," *Bull. Am. Phys. Soc*., 61(20), 174; 69th Annual Meeting of APS/DFD, 20-22 November 2016, Portland, Oregon.
2. Hammer, P., Visbal, M,. Naguib, A., and Koochesfahani, M. [2016] "Lift on a Steady Airfoil in Low Reynolds Number Shear Flow," *Bull. Am. Phys. Soc*., 61(20), 173; 69th Annual Meeting of APS/DFD, 20-22 November 2016, Portland, Oregon.
3. Safaripour, A., Olson, D., Naguib, A., and Koochesfahani, M. [2016] "On Using Shaped Honeycombs for Experimental Generation of Arbitrary Velocity Profiles in Test Facilities," *Bull. Am. Phys. Soc*., 61(20), 265; 69th Annual Meeting of APS/DFD, 20-22 November 2016, Portland, Oregon.
4. Hammer, P., Barnes, C., Visbal, M., Naguib, A., and Koochesfahani, M. [2017] "Effect of Reynolds Number on the Lift on a Steady Airfoil in Uniform Shear Flow," *Bull. Am. Phys. Soc*., 62(14), Abs: A17.00001; 70th Annual Meeting of APS/DFD, 19-21 November 2017, Denver, Colorado.

*5.C. Planned Presentations*

1. Olson, D., Naguib, A. and Koochesfahani, M. [2018] "The effect of steady shear on the aerodynamic performance of an airfoil at low Reynolds number," *71th Annual Meeting of the APS Division of Fluid Dynamics*, Atlanta, GA.
2. Hammer, P., Naguib, A. and Koochesfahani, M. [2018] "Vortical airfoil wake structure in non-uniform approach flow," *71th Annual Meeting of the APS Division of Fluid Dynamics*, Atlanta, GA.
3. Safaripour, A., Naguib, A., and Koochesfahani, M. [2018] "Aerodynamic forces on a steady airfoil in a two-stream shear layer," *71th Annual Meeting of the APS Division of Fluid Dynamics*, Atlanta, GA



DISTRIBUTION A: Distribution approved for public release

*5.D. Journal Manuscripts in Preparation*

We are presently preparing five manuscripts for journal publication: one paper is based on conference paper #2 in §5.*A.*, the second presents the shear generation methodology, the third focuses on the experimental verification of the phenomenon of negative lift at zero AoA, the fourth discusses the Reynolds number dependence of negative lift at zero AoA, and the fifth outlines the results for the two-stream shear layer approach flow.

## 6. Personnel

Research conducted in this project was carried out by three PhD students and one postdoctoral researcher under the supervision of Koochesfahani and Naguib. The postdoctoral researcher Dr. Patrick Hammer, who was partially supported by this grant, is responsible for the computational portions of this work. The PhD students were David Olson, Alireza Safaripour, and Mitchell Albrecht. David Olson obtained his PhD in December 2017 and continued to work on this project as a postdoctoral researcher with support from non-AFOSR funds. Alireza Safaripour, who has been partially supported by this grant, is continuing his PhD research on the influence of two-stream shear layer approach flow on airfoil aerodynamics even though the grant has ended. Mitchell Albrecht contributed to certain aspects of this project early on but was not funded by AFOSR. He is an NDSEG Fellow.

## 7. Summary

A coordinated experimental and computational investigation is carried out to determine how the basic flow physics of steady and unsteady airfoils are altered when the upstream approach flow is changed from the traditional uniform conditions to that of non-uniform flow. Our particular objectives are to establish the alterations that occur for both the load on the airfoil and also the flow field structure. Two classes of canonical flows are considered as our upstream boundary condition: 1) approach flow with linear velocity profile (i.e. uniform shear rate), which also provides a connection to Tsien's inviscid theory, and 2) the plane two-stream shear layer. In this study we consider the unsteady NACA 0012 airfoil in pure pitch with low to moderate angle of attack amplitudes about zero mean angle of attack, and chord Reynolds number of order $10^4$.

The following list summarizes the key outcomes of the study to date:

- A design methodology was developed, based on an extension of existing work for generation of linear profile (uniform shear), that allows us to create velocity profiles of arbitrary shape inside a wind/water tunnel. In this methodology based on shaped honeycombs, the variable-length honeycomb profile shape is computed to create the appropriate pressure drop variation that results in the desired velocity profile downstream of the honeycomb.
- Capability was developed for high accuracy steady and unsteady load measurements on stationary and moving airfoils in the water tunnel.
- Computational capability of *FDL3DI* solver was extended to allow computation of steady and unsteady aerodynamics with non-uniform approach flow.



DISTRIBUTION A: Distribution approved for public release

- Both computations and experiments show that the steady NACA 0012 airfoil at zero AoA generates *negative* lift when placed inside a steady approach flow with uniform positive shear. This finding is *in opposite direction* of the prediction from Tsien's inviscid theory for lift generation in the presence of positive shear. A hypothesis is formulated to explain the observed sign of the lift force on the basis of the asymmetry in boundary layer development on the upper and lower surfaces of the airfoil, which creates an effective airfoil shape with negative camber. The resulting scaling of the viscous effect with shear rate and Reynolds number is provided. Several other interesting flow field asymmetries that develop due to imposed shear are quantified. They include the location of leading edge stagnation point, the location of boundary layer separation point on the airfoil's upper and lower surfaces, and the wake vortical structure.
- Results of computations and experiments for the unsteady airfoil placed inside a steady approach flow with uniform positive shear reveal several interesting new phenomena. At high enough oscillation reduced frequency the vortical wake pattern deflects upward towards the high-speed side of shear profile. The mean lift force, which is zero in uniform freestream, becomes positive above a certain reduced frequency due to the asymmetry caused by upstream shear. The magnitude of this lift force increases with both shear rate and oscillation reduced frequency. On the other hand, lift fluctuation is not affected and stays identical to that in uniform flow. The mean and fluctuating thrust force are also weakly affected by upstream shear for the cases studied here. It is noteworthy that the generation of non-zero lift does not coincide with the development of a deflected wake. Moreover, for cases where the wake does deflect, the sign of the lift is contrary to that expected from the wake deflection direction. Further analysis of data is ongoing in order to gain a better understanding of the observed phenomena.
- When the upstream approach flow is changed to the unsteady flow created by a two-stream shear layer, experiments show that the steady NACA 0012 airfoil at zero AoA generates *positive* lift. This outcome is opposite of what was found earlier for the case of steady approach flow with uniform positive shear. In addition, the character of the ($C_L$ - $\alpha$) curve is fundamentally different with the two-stream shear layer as upstream approach flow. The multi-slope features of the curve in the case of uniform flow completely disappear in favor of a much longer linear region characteristic of much higher Reynolds number airfoils. There is also a much larger increase in the lift coefficient at high angles of attack, with the largest change occurring in the negative AoA region. The underlying physical mechanisms behind these intriguing results are currently under examination.
- In the case of unsteady airfoil placed inside the two-stream shear layer, many of the general features of the load on the airfoil are similar to those discovered for the case of steady shear flow as the approach stream. For example, the mean lift starts to increase above the steady airfoil lift once the oscillation reduced frequency is beyond a certain value, with the magnitude of additional lift increasing with the oscillation reduced frequency. Interestingly, the lift fluctuation variation with reduced frequency is not affected by the form of upstream boundary condition; two-stream shear layer, steady shear flow, and uniform freestream all lead to nearly identical lift fluctuation level at a given reduced frequency. Similarly, the mean thrust and its fluctuation level are weakly affected by the upstream boundary conditions we have studied here.



DISTRIBUTION A: Distribution approved for public release

## References:


1. Theodorsen, T. [1935] "General theory of aerodynamic instability and the mechanism of flutter," NACA TR 496.
2. Von Karman, T. and Sears, W. R. [1938] "Airfoil theory for non-uniform motion," *Journal of the Aeronautical Sciences*, Vol. 5, No. 10, 379-390.
3. Giesing, J. P. [1968] "Nonlinear two-dimensional unsteady potential flow with lift," *J. Aircraft*, Vol. 5, No. 2, 135-143.
4. Djojodihardjo, R. H. and Widnall, S. E. [1969] "A numerical method for the calculation of nonlinear, unsteady lifting potential flow problems," *AIAA J.*, Vol. 7, No. 10, 2001-2009
5. Vezza, M. and Galbraith, R. A. McD. [1985] "A method for predicting unsteady potential flow about an airfoil, "*International Journal for Numerical Methods in Fluids*, Vol. 5, 347-356.
6. Koochesfahani, M. M. [1989] "Vortical patterns in the wake of an oscillating airfoil," *AIAA J.*, Vol. 27, No. 9, 1200-1205.
7. Lai, J. C. S. and Platzer, M. F. [1999] "Jet characteristics of a plunging airfoil," *AIAA J.*, Vol. 37, No. 12, 1529-1537.
8. Young, J. and Lai, J. C. S. [2004] "Oscillation frequency and amplitude effects on the wake of a plunging airfoil," *AIAA J.*, Vol. 42, No. 10.
9. Anderson, J. M., Streitlien, K., Barrett, D. S. and Triantafyllou, M. S. [1998] "Oscillating foils of high propulsive efficiency," *J. Fluid Mech.*, Vol. 360, 41-72.
10. Ol, M. V. [2007] "Vortical structures in high frequency pitch and plunge at low Reynolds number," AIAA-2007-4233.
11. Bohl, D. G. and Koochesfahani, M. M. [2009] "MTV Measurements of the Vortical Field in the wake of an Airfoil Pitching at High Reduced Frequency," *J. Fluid Mech.*, Vol. 620, 63-88.
12. Visbal, M. R. [1986] "Evaluation of an implicit Navier-Stokes solver for some unsteady separated flows," *AIAA* Paper No. AIAA-86-1053.
13. 15. Visbal, M. R. and Shang, J. S. [1989] "Investigation of the flow structures around a rapidly pitching airfoil," *AIAA J.*, **27(8)**.
14. Stanek, M. J. and Visbal, M. R. [1989] "Study of the vortical wake patterns of an oscillating airfoil" *AIAA* Paper No. AIAA-89-0554.
15. Gendrich, C. P., Koochesfahani, M. M. and Visbal, M. R. [1995] "Effects of initial acceleration on the flow field development around rapidly pitching airfoils," *J. Fluids Engineering*, Vol. 117, 45-49.
16. 13. Ramamurti, R. & Sandberg, W. [2001] "Simulation of flow about flapping airfoils using finite element incompressible flow solver," *AIAA J.*, Vol. 39, 253.
17. Shyy, W., Lian, Y., Tang, J., Liu, H., Trizila, P., Stanford, B., Bernal, L., Cesnik, C., Friedmann, P, and Ifju, P. [2008] "Computational aerodynamics of low Reynolds number plunging, pitching and flexible wings for MAV applications," *AIAA* Paper No. AIAA-2008-523.
18. Yu, M.L., Hu, H., and Wang, Z. J. [2010] "A Numerical Study of Vortex-Dominated Flow around an Oscillating Airfoil with High-Order Spectral Difference Method," AIAA 2010-726.
19. Jee, S., and Moser, R.D. [2012] "Conservative Integral Form of the Incompressible Navier-Stokes Equations for a Rapidly Pitching Airfoil," *J. Comp. Phys.*, Vol. 231, 6268-6289.
20. Leishman, G. J. [2006] **Principles of Helicopter Aerodynamics**, Cambridge Aerospace Series.
21. Tsien, H-S. [1943] "Symmetrical Joukowsky Airfoils in Shear Flow," *Q. Appl. Math*, Vol. 1, pt. 2, 130-148.




DISTRIBUTION A: Distribution approved for public release

22. James, D. G. [1951] "Two-Dimensional Airfoils in Shear Flow," *Quart. Journ. Mech. and Applied Math*, Vol. IV, pt. 4, 407-418.
23. Honda, M. [1960] "Theory of a Thin Wing in a Shear Flow," *Proceedings of the Royal Society of London. Series A, Mathematical and Physical Sciences*, Vol. 254, No. 1278, 372-394.
24. Nishiyama, T., and Hirano, K. [1970] "Aerofoil Section Characteristics in Shear Flows," *Ingenieur-Archiv*, Vol. 39, pt. 3, 137-148.
25. Payne, F., and Nelson, R. [1985] "Aerodynamic characteristics of an airfoil in a nonuniform wind profile," *J. Aircraft*, **22(1)**, 5-10.
26. Elder, J. [1959] "Steady flow through non-uniform gauzes of arbitrary shape," *J. Fluid Mech*., **5(03)**, 355.
27. Owen, P. R. and Zienkiewicz, H. K. [1957] "The production of uniform shear flow in a wind tunnel," *J. Fluid Mech*., Vol. 2, 521–531.
28. Kotansky, D. R. [1966] "The use of honeycomb for shear flow generation," *AIAA J*., **4(8)**, 1490–1491.
29. Safaripour, A., Olson, D., Naguib, A., and Koochesfahani, M. [2016] "On Using Shaped Honeycombs for Experimental Generation of Arbitrary Velocity Profiles in Test Facilities," *Bull. Am. Phys. Soc*., 61(20), 265; 69th Annual Meeting of APS/DFD, 20-22 November 2016, Portland, Oregon.
30. Liepmann, H. W., and Laufer, J. [1947] "Investigations of Free Turbulent Mixing," *NACA Tech. Note*, no. 1257.
31. Wygnanski, I., and Fiedler, H. E. [1970] "The two-dimensional mixing region," *J. Fluid Mech.*, **41(02)**, 327.
32. Brown, G. L., and Roshko, A. [1974] "On density effects and large structure in turbulent mixing layers," *J. Fluid Mech.*, **64(04)**, 775.
33. Olson, D., Naguib, A., and Koochesfahani, M. [2016] "Experiments on a Steady Low Reynolds Number Airfoil in a Shear Flow," *Bull. Am. Phys. Soc*., 61(20), 174; 69th Annual Meeting of APS/DFD, 20-22 November 2016, Portland, Oregon.
34. Gaitonde, D., and Visbal, M. [1998] "High-order schemes for Navier-Stokes equations: algorithm and implementation into FDL3DI," *Air Force Research Laboratory AFRL-VA-WP-TR-1998-3060*, Wright-Patterson Air Force Base, Ohio.
35. Visbal, M. R., and Gaitonde, D. V. [1999] "High-order-accurate methods for complex unsteady subsonic flows," *AIAA J.*, **37 (10)**, 1231-1239.
36. Lele, S. [1992] "Compact finite difference schemes with spectral-like resolution," *J. Comp. Phys*., **103(1)**, 16-42.
37. Beam, R., and Warming, R. [1978] "An implicit factored scheme for the compressible Navier-Stokes equations," *AIAA J.,***16**(4), 393-402.
38. Pulliam, T., and Chaussee, D. [1981] "A diagonal form of an implicit approximate- factorization algorithm," *J. Comp. Phys.*, **39**(2), 347-363.
39. Visbal, M., and Gaitonde, D. [2002] "On the use of higher-order finite difference schemes on curvilinear and deforming meshes," *J. Comp. Phys.,* **181**, 155-185.
40. Visbal, M., Morgan, P., and Rizzetta, D. [2003] "An Implicit LES Approach Based on High-Order Compact Differencing and Filtering Schemes (Invited)", *AIAA* Paper 2003-4098, 16th AIAA Computational Fluid Dynamics Conference, Fluid Dynamics and Conferences, Orlando, FL.



DISTRIBUTION A: Distribution approved for public release

41. Hammer, P. [2016] "Computational study on the effect of Reynolds number and motion trajectory asymmetry on the aerodynamics of a pitching airfoil at low Reynolds number," *PhD thesis*, Department of Mechanical Engineering, Michigan State University, East Lansing, Michigan.
42. Hammer, P., Visbal, M,. Naguib, A., and Koochesfahani, M. [2016] "Lift on a Steady Airfoil in Low Reynolds Number Shear Flow," *Bull. Am. Phys. Soc*., 61(20), 173; 69th Annual Meeting of APS/DFD, 20-22 November 2016, Portland, Oregon.
43. Hammer, P., Visbal, M., Naguib, A., Koochesfahani, M. [2018] "Lift on a steady 2-D symmetric airfoil in viscous shear flow," *J. Fluid Mech*., **837**, R2 (11 pp) (doi:10.1017/jfm.2017.895)
44. Hammer, P. R., Olson, D. A., Visbal, M. R., Naguib, A. M., and Koochesfahani, M. M. [2018] "An Investigation of the Aerodynamics of a Harmonically Pitching Airfoil in Uniform-Shear Approach Flow," *AIAA* Paper No. AIAA 2018-0575.
45. Hammer, P., Barnes, C., Visbal, M., Naguib, A., and Koochesfahani, M. [2017] "Effect of Reynolds Number on the Lift on a Steady Airfoil in Uniform Shear Flow," *Bull. Am. Phys. Soc*., 62(14), Abs: A17.00001; 70th Annual Meeting of APS/DFD, 19-21 November 2017, Denver, Colorado.
46. Yu, M., Wang, B., Wang, Z. J., and Farokhi, S. [2018] "Evolution of Vortex Structures over Flapping Foils in Shear Flow and its Impact on Aerodynamic Performance," *Journal of Fluids and Structures*, Vol. 75, pp. 116-134.
47. Cleaver, D. J., Wang, Z. J. and Gursul, I. [2012] "Bifurcating Flows of Plunging Aerofoils at High Strouhal Numbers," *J. Fluid Mech.*, Vol. 708, pp. 349-376.



DISTRIBUTION A: Distribution approved for public release

# AFOSR Deliverables Submission Survey

Response ID:10335 Data

1.

**Report Type**

Final Report

**Primary Contact Email**

**Contact email if there is a problem with the report.**

koochesf@egr.msu.edu

**Primary Contact Phone Number**

**Contact phone number if there is a problem with the report**

517-353-5311

**Organization / Institution name**

Michigan State University

**Grant/Contract Title**

**The full title of the funded effort.**

Canonical Shear Flow Interactions with Unsteady Airfoils

**Grant/Contract Number**

**AFOSR assigned control number. It must begin with "FA9550" or "F49620" or "FA2386".**

FA9550-15-1-0224

**Principal Investigator Name**

**The full name of the principal investigator on the grant or contract.**

Manoochehr Koochesfahani

**Program Officer**

**The AFOSR Program Officer currently assigned to the award**

Dr. Gregg Abate

**Reporting Period Start Date**

06/15/2015

**Reporting Period End Date**

06/14/2018

**Abstract**

A coordinated experimental and computational investigation is carried out to determine how the basic flow physics of steady and unsteady airfoils are altered when the upstream approach flow is changed from the traditional uniform conditions to that of non-uniform flow. Our particular objectives are to establish the alterations that occur for both the load on the airfoil and also the flow field structure. This work considers the NACA 0012 airfoil in pure pitch with low to moderate angle of attack amplitudes about zero mean angle of attack, and chord Reynolds number of order 10,000. It is found that a steady symmetric airfoil has negative lift at zero angle of attack when placed in steady shear flow with positive shear, opposite of the prediction of inviscid theory. A hypothesis is formulated to explain the observed sign of the lift force on the basis of the asymmetry in boundary layer development on the upper and lower surfaces of the airfoil, which creates an effective airfoil shape with negative camber. However, it is found that the same steady airfoil placed in the unsteady flow field of a two-stream shear layer generates positive lift at zero angle of attack. Also, the character of the (CL - alpha) curve changes fundamentally and the multi-slope features of the curve in the case of uniform flow completely disappear in favor of a much longer linear region characteristic of much higher Reynolds number airfoils. The main influence of shear approach flow on unsteady aerodynamic

DISTRIBUTION A: Distribution approved for public release

load is on the mean lift, leaving the mean thrust and force fluctuations mostly unaffected.

**Distribution Statement**

**This is block 12 on the SF298 form.**

Distribution A - Approved for Public Release

**Explanation for Distribution Statement**

**If this is not approved for public release, please provide a short explanation. E.g., contains proprietary information.**

**SF298 Form**

**Please attach your SF298 form. A blank SF298 can be found here. Please do not password protect or secure the PDF The maximum file size for an SF298 is 50MB.**

SF_298_AFOSR_AF9550-15-1-0224.pdf

**Upload the Report Document. File must be a PDF. Please do not password protect or secure the PDF . The maximum file size for the Report Document is 50MB.**

Final_Report_AFOSR_AF9550-15-1-0224.pdf

**Upload a Report Document, if any. The maximum file size for the Report Document is 50MB.**

**Archival Publications (published) during reporting period:**

1. Hammer, P., Visbal, M., Naguib, A., Koochesfahani, M. [2018] "Lift on a steady 2-D symmetric airfoil in viscous shear flow," J. Fluid Mech., 837, R2 (11 pp) (doi:10.1017/jfm.2017.895)

2. Hammer, P. R., Olson, D. A., Visbal, M. R., Naguib, A. M., and Koochesfahani, M. M. [2018] "An Investigation of the Aerodynamics of a Harmonically Pitching Airfoil in Uniform-Shear Approach Flow," AIAA Paper No. AIAA 2018-0575.

**New discoveries, inventions, or patent disclosures:**

**Do you have any discoveries, inventions, or patent disclosures to report for this period?**

No

**Please describe and include any notable dates**

**Do you plan to pursue a claim for personal or organizational intellectual property?**

**Changes in research objectives (if any):**

No Changes.

**Change in AFOSR Program Officer, if any:**

Program officer was originally Dr. Douglas Smith.
Dr. Gregg Abate took over in July of 2018.

**Extensions granted or milestones slipped, if any:**

**AFOSR LRIR Number**

**LRIR Title**

**Reporting Period**

**Laboratory Task Manager**

**Program Officer**

**Research Objectives**

**Technical Summary**

**Funding Summary by Cost Category (by FY, $K)**

| | Starting FY | FY+1 | FY+2 |
|---|---|---|---|
| Salary | | | |
| Equipment/Facilities | | | |
| Supplies | | | |
| Total | | | |

**Report Document**

**Report Document - Text Analysis**

**Report Document - Text Analysis**

**Appendix Documents**

## 2. Thank You

**E-mail user**

Sep 13, 2018 10:35:32 Success: Email Sent to: koochesf@egr.msu.edu